A Ferrocene−C_{60}−Dinitrobenzene Triad: Synthesis and Computational, Electrochemical, and Photochemical Studies

Francis D'Souza,*,† Melvin E. Zandler,† Phillip M. Smith,† Gollapalli R. Deviprasad,† Klykov Arkady,† Mamoru Fujitsuka,‡ and Osamu Ito*,‡

Department of Chemistry, Wichita State University, 1845 Fairmount, Wichita, Kansas 67260-0051, and Institute of Multidisciplinary Research for Advanced Materials, Chemical Reaction Science, Tohoku University, Katahira, Sendai, 980-8577 Japan

Received: September 27, 2001; In Final Form: November 12, 2001

Synthesis and physicochemical characterization of a molecular triad comprised of ferrocene, C_{60}, and dinitrobenzene entities is reported. Electrochemical studies revealed multiple redox processes involving all three redox active, ferrocene, C_{60}, and dinitrobenzene entities. A total of eight reversible redox couples within the accessible potential window of *o*-dichlorobenzene containing 0.1 M $(TBA)ClO_4$ are observed. A comparison between the measured redox potentials with those of the starting compounds revealed absence of any significant electronic interactions between the different redox entities. The geometric and electronic structure of the triad is elucidated by using ab initio B3LYP/3-21G(*) methods. In the energy optimized structure, as predicted by electrochemical studies, the first HOMO orbitals are found to be located on the ferrocene entity, whereas the first LUMO orbitals are mainly on the C_{60} entity with small orbital coefficients on the dinitrobenzene entity. The subsequent LUMO's track the observed site of electrochemical reductions of the triad. The photochemical events in the triad are probed by both steady-state and time-resolved techniques. The steady-state emission spectra of the triad and the starting dyad, 2-(ferrocenyl)fulleropyrrolidine, are found to be completely quenched compared to fulleropyrrolidine bearing no redox active substituents. The subpicosecond and nanosecond transient absorption spectral studies reveal efficient charge separation in the triad. As suggested by the coefficients of the LUMO orbitals, the transient absorption spectrum of the triad revealed bands corresponding to the formation of the fulleropyrrolidine anion species. The estimated rise and decay rate constants are found to be 2.5×10^{11} and 8.5×10^{9} s^{-1} for the triad, and these values compare with a rise and decay rate constants of 2.2×10^{11} and 4.5×10^{9} s^{-1} for the ferrocene−C_{60} dyad in benzonitrile. The observed faster rate constants are attributed to the close spacing of the redox entities of the triad to one another.

Introduction

Fullerenes, C_{60} and C_{70}, linked to multiple redox- and/or photoactive molecular entities[1−5] are useful candidates to build molecular/supramolecular electronic devices[6−11] and artificial light energy harvesting systems.[12−26] Toward this, electron donors such as porphyrin, ferrocene, *N*,*N*-dimethylaminophenyl, ruthenium(II) trisbipyridine, and tetrathiafulvarene have been employed to form fullerene−electron donor type dyads, whereas electron acceptors such as benzoquinone derivatives, spiro-annelated methano groups, cyano groups, fluorine atoms, TCNQ and DCNQI derivatives, ammonium cations, and nitroaromatic substituents have been employed to form covalently linked fullerene-electron acceptor type dyads.[1−5,26−28] In addition, a few triads and tetrads bearing one or more different electron donor and/or acceptor entities have been elegantly designed, synthesized, and studied.[15,26−31] Much important and useful information has been obtained from studies involving these molecular and supramolecular systems.

In the present study, we report on the synthesis and physicochemical characterization of a ferrocene−C_{60}−dinitrobenzene, that is, a donor−(acceptor 1)−(acceptor 2)-type triad (Figure 1). Earlier, several groups including us have reported on ferrocene−C_{60} (donor−acceptor)[32−36] and C_{60}−dinitrobenzene (acceptor−acceptor)[37−38] type dyads. The presently developed molecular system combines these two dyads to form a hybrid triad bearing three redox active entities. The geometric and electronic structure of this newly developed triad has been elucidated from optical absorption, electrochemical, and ab initio B3LPY/3-21G(*) methods. Using steady-state and time-resolved emission techniques, the excited-state photoinduced electron-transfer reactions are also probed in the triad.

Experimental Section

Chemicals. Buckminsterfullerene, C_{60} (+99.95%), was from BuckyUSA (Bellaire, TX). *o*-Dichlorobenzene in sure seal bottle, ferrocenaldehyde, 3,5-dinitrobenzoyl chloride, glycine, and tetra-*n*-butylammonium perchlorate, $(TBA)ClO_4$, were from Aldrich Chemicals (Milwaukee, WI). All chemicals were used as received unless otherwise stated. *o*-Dichlorobenzene for electrochemical studies was dried over CaH_2 and distilled under vacuum prior to the experiments. $(TBA)ClO_4$ was recrystallized from ethanol and dried in a vacuum oven at 35 °C for 10 days.

Synthesis. *2-(Ferrocenyl)fulleropyrrolidine*. This was synthesized according to a general procedure developed for the preparation of substituted fulleropyrrolidines based on 1,3-dipolar cycloaddition of azomethine ylides to C_{60}.[33,39] For this, a mixture of C_{60} (100 mg), glycine (53 mg), and ferrocenalde-

* To whom correspondence should be addressed.
† Wichita State University.
‡ Tohoku University.

10.1021/jp0136415 CCC: $22.00
Published on Web 01/04/2002

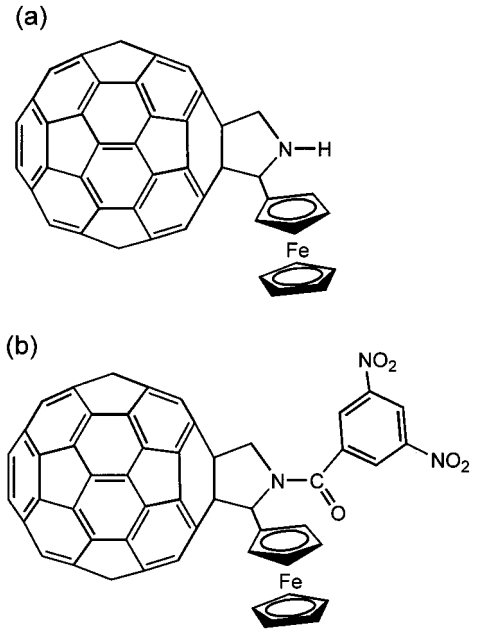

Figure 1. Structure of the investigated (a) 2-(ferrocenyl)fulleropyrrolidine dyad and (b) *N*-(3′,5′-dinitrobenzoyl)-2-(ferrocenyl)fulleropyrrolidine triad.

hyde (75 mg) was refluxed in toluene for 6 h. The compound was purified over silica gel column using toluene/hexane (90:10 v/v) as eluent. Yield 23%. ^{1}H NMR in $CDCl_3/CS_2$ (1:1 v/v), δ ppm, 5.57 (s, 1H, pyrrolidine H), 5.01, 4.88 (d, d, 2H, pyrrolidine H), 4.55, 4.46, 4.21 (s, s, s, 1H, 1H, 2H, ferrocene H), 4.36 (s, 5H, ferrocene H). The ^{13}C NMR spectrum in $CDCl_3/CS_2$ (1:2 v/v) revealed all of the expected peaks.[33] UV−visible in *n*-hexane, λ_{max} nm, 245 (sh), 255, 307 (br), 325, 429. ESI mass in CH_2Cl_2: calcd, 947.65; found, 947.1.

N-(3′,5′-Dinitrobenzoyl)-2-(ferrocenyl)fulleropyrrolidine. This was synthesized by reacting 2-(ferrocenyl)fulleropyrrolidine (50 mg) and an excess of 3,5-dinitrobenzoyl chloride in CH_2Cl_2 containing triethylamine (1.1 eq) for 3 h. The compound was purified over silica gel column using toluene/ethyl acetate (90:10 v/v) as eluent. Yield 38%. ^{1}H NMR in $CDCl_3/CS_2$ (1:1 v/v), δ ppm, 9.19 (s, 1H, dinitrobenzoyl H), 9.14 (s, 2H, dinitrobenzoyl H), 5.57 (s, 1H, pyrrolidine H), 5.01, 4.88 (d, d, 2H, pyrrolidine H), 4.50, 4.21 (m, 4H, ferrocene H), 4.36 (s, 5H, ferrocene H). UV−visible in *n*-hexane, λ_{max} nm, 221, 254 (sh), 309, 326 (br), 414 (br). ESI mass in CH_2Cl_2: calcd, 1141.67; found, 1141.1.

Instrumentation. The UV−visible spectral measurements were carried out with a Shimadzu model 1600 UV-visible spectrophotometer. The fluorescence was monitored by using a Spex Fluorolog tau-3 spectrometer. A right angle detection method was used. The ^{1}H NMR studies were carried out on a Varian 400 MHz spectrometer. Tetramethylsilane (TMS) was used as an internal standard. Cyclic voltammograms were obtained by using a conventional three electrode system on a model AFCB1 bipotentiostat of Pine Instrument Co. (Grove City, PA). A platinum disk electrode was used as the working electrode. A platinum wire served as the counter electrode. An Ag/AgCl electrode, separated from the test solution by a fritted supporting electrolyte/solvent bridge, was used as the reference electrode. The potentials were referenced to an internal ferrocene/ferrocenium redox couple. All of the solutions were purged prior to spectral and electrochemical measurements using argon gas.

Computational Calculations. The computational calculations were performed by using either Gaussian 98,[40] SPARTAN,[41] or Cache MOPAC[42] software packages. The graphics of the HOMO and LUMO molecular orbital coefficients were generated with the help of GaussView software. The compounds were fully optimized to a stationary point on the Born-Openheirmer potential energy surface. The frontier HOMO and LUMO molecular orbital coefficients were calculated on the fully optimized structures.

Time-Resolved Absorption Measurements. The subpicosecond transient absorption spectra were recorded by the pump and probe method. The samples were excited with a second harmonic generation (SHG, 388 nm) of output from a femtosecond Ti:sapphire regenerative amplifier seeded by SHG of a Er-dropped fiber (Clark-MXRCPA-2001 plus, 1 kHz, fwhm 150 fs). The excitation light was depolarized. The monitor white light was generated by focusing the fundamental of laser light on the flowing D_2O/H_2O cell. The transmitted monitor light was detected with a dual MOS linear image sensor (Hamamatsu Photonics, C6140) or InGaAs photodiode array (Hamamatsu Photonics, C5890-128).

Nanosecond transient absorption spectra in the NIR region were measured by means of laser-flash photolysis; 532 nm light from a Nd:YAG laser was used as the exciting source, and a Ge-avalanche-photodiode module was used for detecting the monitoring light from a pulsed Xe lamp as described in our previous report.[43−45]

Results and Discussion

The procedure developed for the synthesis of the triad bearing three different redox active entities, namely, ferrocene, C_{60}, and dinitrobenzene, is found to be an elegant one. The method of covalent linking dinitrobenzoyl entity to the fulleropyrrolidine nitrogen is not much different from the earlier reported Sanger's reaction which involved a direct reaction between the fulleropyrrolidine secondary nitrogen and 1-fluoro-2,4-dinitrobenzene.[37] The ESI mass spectrum of the triad in the CH_2Cl_2 matrix revealed the molecular ion peak in agreement with the calculated one. The integrated peak intensities of the ^{1}H NMR spectrum clearly established the molecular integrity of the triad. The resonance peak positions of the pyrrolidine and ferrocene entities were found at positions almost identical to that of the starting material, 2-ferrocenylfulleropyrrolidine. Only the dinitrobenzoyl proton resonance peaks revealed a small shielding (0.1−0.2 ppm) as compared to its starting material, 3,5-dinitrobenzoyl chloride. The optical absorption spectrum of the triad exhibited absorption bands corresponding to the C_{60} and dinitrobenzoyl entities. The absorption peaks corresponding to the ferrocene entity were merged into the strong absorption bands of C_{60} and dinitrobenzoyl entities in the 225−425 nm wavelength region.

Cyclic Voltammetric Studies. Electrochemical studies using the cyclic voltammetric technique have been performed to evaluate potentials of the different redox active entities and also to visualize any electronic interactions between them. Figure 2 shows the cyclic voltammograms of 2-(ferrocenyl)fulleropyrrolidine and *N*-(3′,5′-dinitrobenzoyl)-2-(ferrocenyl)-fulleropyrrolidine in dry *o*-dichlorobenzene containing 0.1 M $(TBA)ClO_4$. For 2-(ferrocenyl)fulleropyrrolidine, the reversible redox potential corresponding to the oxidation of the ferrocene entity is located at 0.06 V vs Fc/Fc^+, whereas the potentials for the first three reversible reductions of the C_{60} entity are located at −1.19, −1.57, and −2.11 V vs Fc/Fc^+. The anodic to cathodic peak separations were found to range between 100 and 110 mV and plots of peak current vs square root of scan rates were linear

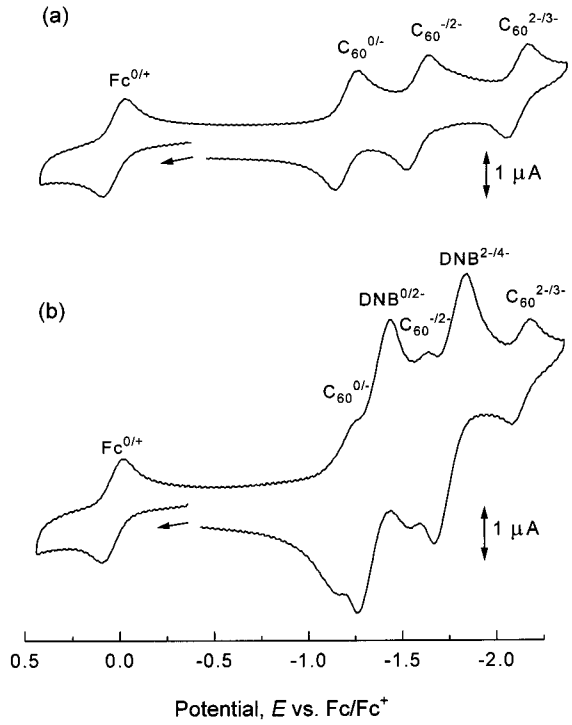

Figure 2. Cyclic voltammograms of (a) 2-(ferrocenyl)fulleropyrrolidine and (b) *N*-(3′,5′-dinitrobenzoyl)-2-(ferrocenyl)fulleropyrrolidine in 0.1 M $(TBA)ClO_4$, *o*-dichlorobenzene. Scan rate = 100 mV/s.

SCHEME 1

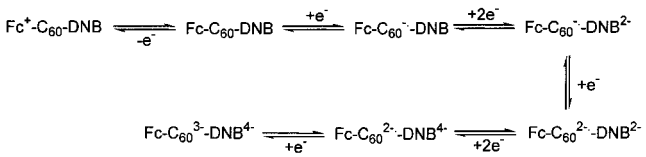

for these redox reactions under the present solution conditions. The measured redox potentials agreed well with the potentials reported earlier for ferrocene linked fullerene derivatives[33] and fulleropyrrolidine derivatives[46] in general.

Interestingly, the voltammogram of the triad exhibited reversible redox processes corresponding to the reduction of the appended dinitrobenzoyl entity, in addition to the ferrocene and C_{60} entities. The electrode processes corresponding to the reduction of the dinitrobenzoyl entity are located at −1.35 and −1.76 V vs Fc/Fc^+. The anodic to cathodic peak separation is found to vary between 160 and 170 mV, and multiple scanning of the voltammograms in the potential range did not change the current or shape of the voltammograms. A comparison between the peak currents for these processes with that of the ferrocene and fullerene redox couples in Figure 2b suggests that each of the redox processes of the dinitrobenzoyl group involves two one-electron reactions, presumably involving simultaneous reduction of the two nitro groups of the dinitrobenzoyl entity. The reversible redox potential corresponding to the appended ferrocene oxidation is located at 0.05 V, whereas the first three reversible fulleropyrrolidine reductions are located at −1.19, −1.58, and −2.13 V vs Fc/Fc^+. An examination of these potentials with that of the starting material, 2-(ferrocenyl)-fulleropyrrolidine in Figure 2a suggests the absence of significant electronic interactions between the different redox entities. The sequence of the occurrence of different electrode reactions in the triad is summarized in Scheme 1, where Fc represents the ferrocenyl entity, C_{60} represents the fulleropyrrolidine entity while, and DNB represents the dinitrobenzoyl entity of the triad.

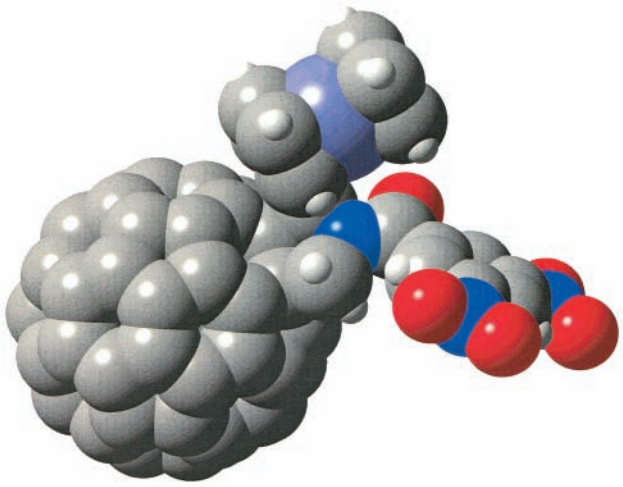

Figure 3. Space filling model of the B3LPY/3-21G(*) optimized structure of *N*-(3′,5′-dinitrobenzoyl)-2-(ferrocenyl)fulleropyrrolidine.

Importantly, the observed eight reversible redox processes (one oxidation and seven reductions) within the accessible potential window of the solvent under ordinary solution conditions are noteworthy. It is now well-known that under special solution conditions, that is, solvents with extended potential window and reduced temperature, pristine fullerenes (C_{60} and C_{70}) exhibit six one-electron reversible reductions.[47] Owing to the presence of a large number of reversible reductions, fullerenes are considered potential candidates to build molecular electronic devices.[4−11] The present triad which undergoes eight reversible redox reactions under ordinary solutions conditions is more appealing in this regard than pristine fullerenes because a large number of reversible redox reactions can be accomplished under normal experimental conditions. Our present results suggest that fullerenes bearing one or more redox active groups undergoing reversible redox reactions are potentially more useful than pristine C_{60} specially to build molecular electronic devices.

Computational Studies

Prediction of the accurate geometric and electronic structure of supramolecular systems bearing one or more different types of redox and/or photoactive groups poses a challenge for researchers working in this area.[48] The geometric parameters are obtained easily by semiempirical PM3 and AM1 methods because these methods possess built-in parameters. However, semiempirical methods often yield errors in the calculated electronic structure. Ab initio calculations based on either density functional theory or Hartree−Fock methods at a moderate level often yield correct geometry and electronic structures which agree with the experimental results. Here, we have utilized both semiempirical PM3 and ab initio methods at the 3-21G(*) level to probe the geometry and electronic structure of the triad.

In the present study, the ab initio calculations at the B3LYP/3-21G(*) level and the HF/3-21G(*) level have been performed using Gaussian 98 software, whereas the semiempirical calculations have been performed using Cache MOPAC or SPARTAN programs. As discussed below, however, only the B3LYP/3-21G(*) methods resulted in the prediction of plausible geometry and electronic structure. Figure 3 shows the space-filling model of the energy minimized structure on the Born−Openheimer potential energy surface, whereas Figure 4 shows the first HOMO and the first five LUMO frontier molecular orbitals. In the optimized structure, the pyrrolidine ring is puckered in such

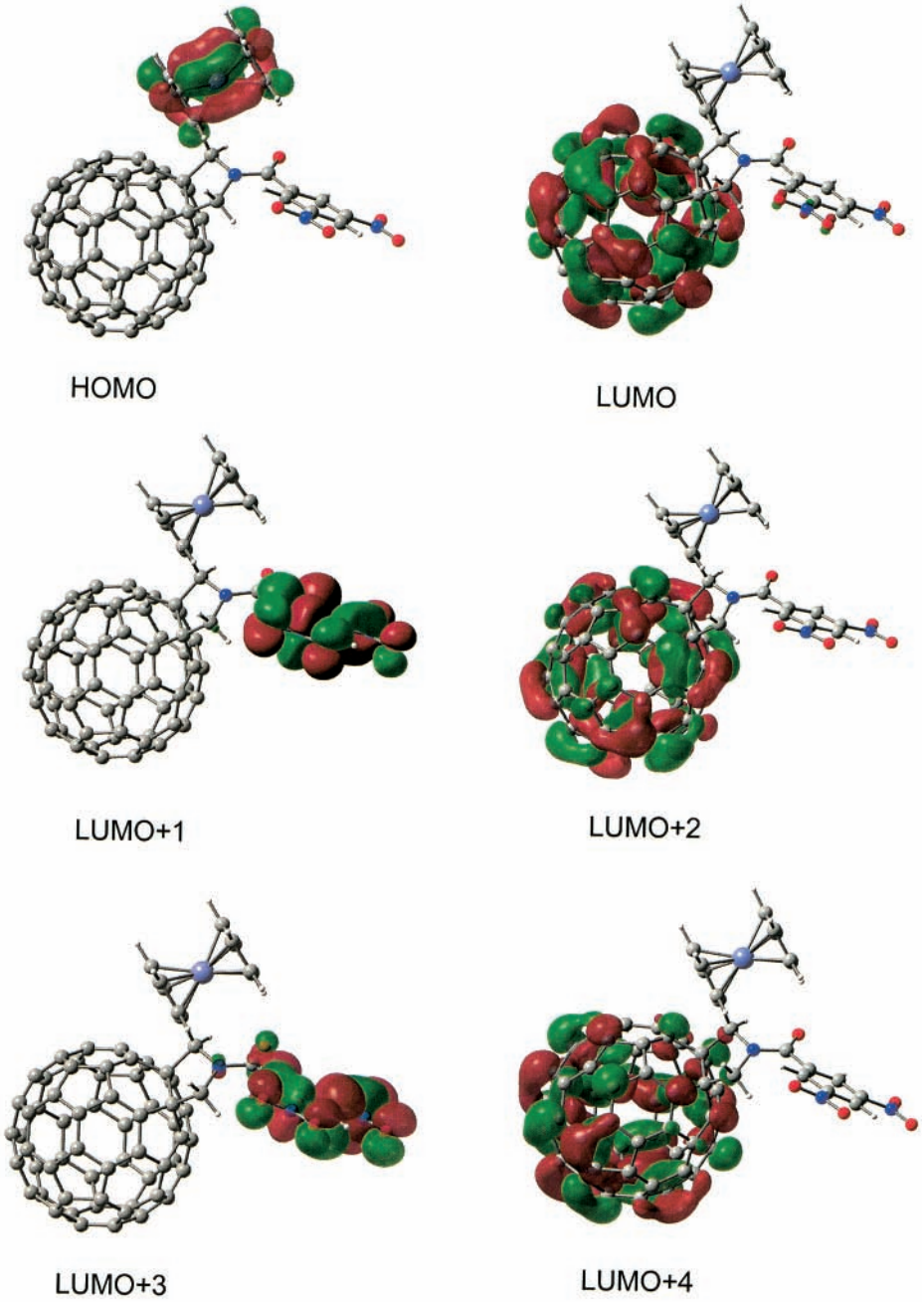

Figure 4. Frontier HOMO, LUMO, LUMO+1, LUMO+2, LUMO+3, and LUMO+4 orbitals of the investigated *N*-(3′,5′-dinitrobenzoyl)-2-(ferrocenyl)fulleropyrrolidine triad.

a way that the 2-ferrocenyl entity is anti to the nitrogen atom and the *N*-dinitrobenzoyl group is trans[49] to the 2-ferrocenyl group. The two nitro groups of the dinitrobenzoyl entity are coplanar with the phenyl ring, whereas the carbonyl group is out of the plane of the dinitrobenzene ring with a dihedral angle of about 25°. The carbonyl group lies along the N−C(ferrocene) bond of the pyrrolidine ring with a dihedral angle of 2°. The two cyclopentadienyl rings of the ferrocene entity form an almost eclipse configuration. The carbon atoms of the 6,6-ring junction from which the pyrrolidine ring is formed are nearly 0.35 Å away from the positions of the normal C_{60} spheroid carbons. Earlier, an X-ray analysis of fulleropyrrolidine in a self-assembled 2-(4′-pyridyl)fulleropyrollidine and tetraphenylporphyrinatozinc(II)[50] had revealed such structural distortions in agreement with calculations at the B3LYP/STO-3G* level. In the energy minimized structure, the center-to-center distance between the C_{60} spheroid and ferrocene entities is found to be 8.28 Å, whereas this difference between the C_{60} spheroid and dinitrobenzoyl entities is around 9.06 Å, and between the ferrocene and dinitrobenzoyl entities, this distance is about 6.50 Å. The edge-to-edge distance between the C_{60} spheroid and ferrocene entities is found to be 2.59 Å, whereas this distance between the C_{60} spheroid and dinitrobenzoyl entities is about 4.32 Å, and between the ferrocene and dinitrobenzoyl entities, this distance is about 4.55 Å.

In agreement with the electrochemical results, the frontier HOMO is found to be located on the ferrocene entity (Figure 4a). Interestingly, as expected from the electrochemical data, the majority of the frontier LUMO is located on the C_{60} spheroid, whereas a small portion of the orbital is also found to exist on one of the nitro groups of the dinitrobenzoyl entity (Figure 4b). The calculated (gas phase) HOMO−LUMO gap is found to be 2.12 eV, and this compares with the electrochemically measured (difference between the first oxidation and

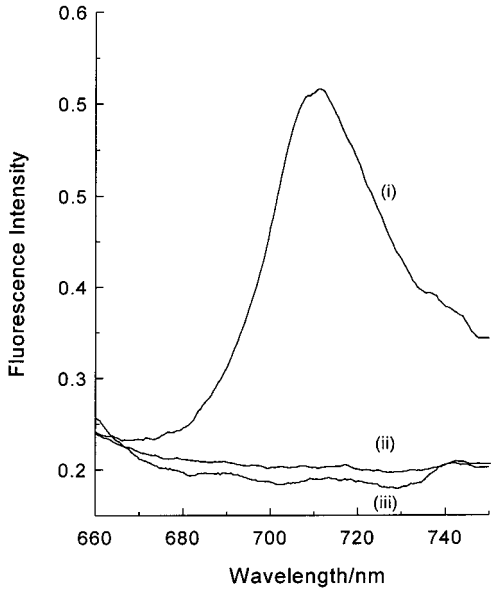

Figure 5. Steady-state fluorescence emission spectrum of (i) 2-(phenyl)fulleropyrrolidine, (ii) 2-(ferrocenyl)fulleropyrolidine, and (iii) *N*-(3′,5′-dinitrobenzoyl)-2-(ferrocenyl)fulleropyrrolidine in *o*-dichlorobenzene; $\lambda_{ex} = 390$ nm. Concentration of fullerenes employed $= 10^{-4}$ M.

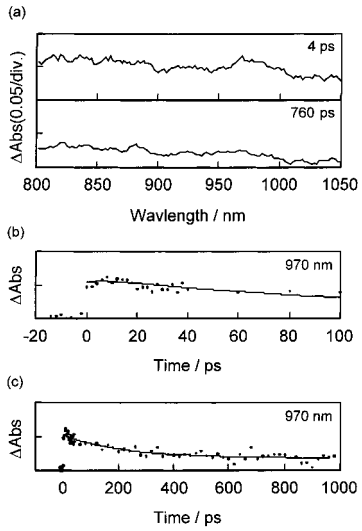

Figure 6. (a) Transient absorption spectra of 2-(ferrocenyl)fulleropyrrolidine in benzonitrile at 4 and 760 ps after the laser irradiation (388 nm, <150 fs). (b and c) Absorption time profiles at 970 nm. Solid lines were fitted curves assuming rise and decay of 2.2×10^{11} and 4.5×10^{9} s^{-1} of rate constants, respectively.

first reduction potential) value of 1.23 V. The orbital energies of the first HOMO and the first five LUMO orbitals are found to be −5.723, −3.597, −3.572, −3.520, −3.343, and −3.239 eV, respectively. The subsequent virtual orbitals, that is, LUMO+1, LUMO+2, LUMO+3, and LUMO+4, are shown in Figures 4c−d. These virtual orbitals are localized as: C_{60}, dinitrobenzene, C_{60}, dinitrobenzene, and C_{60} entities. Interestingly, this trend tracks the sequence of the site of electron transfer of the triad as depicted in Scheme 1. To our knowledge, this is the first example where, in a supramolecular system comprised of three redox entities, the calculated HOMO and virtual orbitals track the observed multistep electrochemical redox reactions. It may be mentioned here that only recently the validity of molecular orbitals generated by density functional methods is being recognized.[51] The accuracy of these methods,

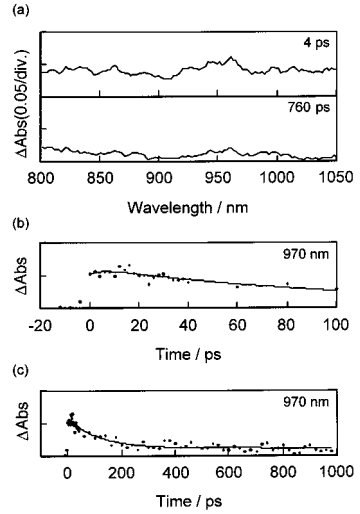

Figure 7. (a) Transient absorption spectra of *N*-(3′,5′-dinitrobenzoyl)-2-(ferrocenyl)fulleropyrrolidine in benzonitrile at 4 and 760 ps after the laser irradiation (388 nm, <150 fs). (b and c) Absorption time profiles at 970 nm. Solid lines were fitted curves assuming rise and decay of 2.5×10^{11} and 8.5×10^{9} s^{-1} of rate constants, respectively.

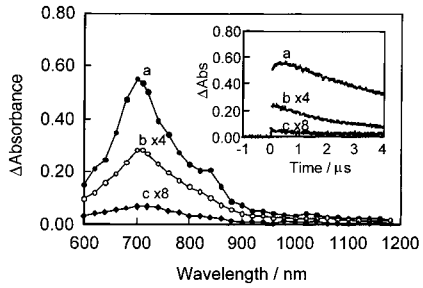

Figure 8. Transient absorption spectra of (a) fulleropyrrolidine, (b) 2-(ferrocenyl)fulleropyrrolidine, and (c) *N*-(3′,5′-dinitrobenzoyl)-2-(ferrocenyl)fulleropyrrolidine in benzonitrile at 100 ns after the laser irradiation (352 nm, 6 ns). Figure inset: absorption time profiles at 720 nm.

especially B3LYP, is recently being demonstrated by Schaefer and co-workers on electron affinities of aromatic compounds.[52]

As mentioned earlier, our attempts using semiempirical PM3 and Hartree−Fock ab initio methods at a 3-21G(*) level resulted either in incorrect geometry or electronic structure for the studied triad. The PM3 calculations using Cache MOPAC revealed a plausible geometry (later used as the starting geometry in the B3LYP and HF calculations) but the HOMO orbitals were found to be on the C_{60} entity. The PM3 calculations performed using SPARTAN revealed at least three stable structures, the two low energy structures had HOMO's on ferrocene, but revealed interactions between the carbonyl group or phenyl ring hydrogens of dinitrobenzoyl entity and the ferrocene iron resulting into a distorted ferrocene (the coplanarity of the two cyclopentadienyl rings was lost). The third SPARTAN structure was similar to the Cache MOPAC structure with HOMO on the fullerene entity. Interestingly, the structure calculated using the Hartree−Fock 3-21G(*) method optimized to a geometry close to the B3LYP structure, but like the Cache MOPAC PM3 results, the HOMO was found to be on the fullerene entity. In the absence of any spectroscopic evidence for such distorted geometry and electronic properties, we did not further use these methods and adopted only the density functional method (B3LYP) where the calculated geometry and electronic properties agreed well with the experimental observations.

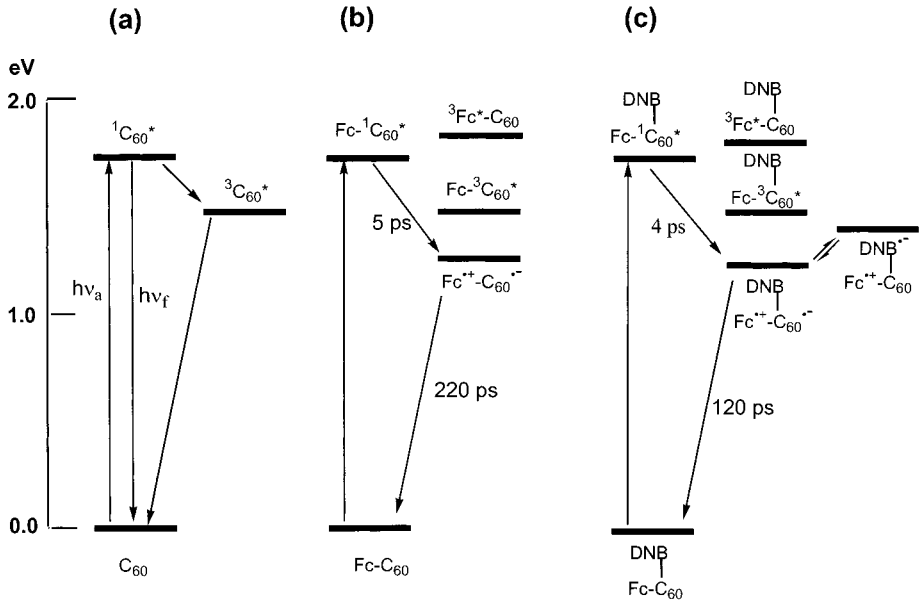

Figure 9. Energy level diagrams of (a) fulleropyrrolidine (C_{60}), (b) 2-(ferrocenyl)fulleropyrrolidine (Fc−C_{60}), and (c) *N*-(3′,5′-dinitrobenzoyl)-2-(ferrocenyl)fulleropyrrolidine (Fc−C_{60}−DNB).

Photochemical Studies. Figure 5 shows the room-temperature fluorescence emission spectra of the 2-(ferrocenyl)fulleropyrrolidine dyad, the ferrocene−C_{60}−dinitrobenzene triad, and a reference compound, 2-(phenyl)fulleropyrrolidine, bearing no ferrocene or dinitrobenzene entities in *o*-dichlorobenzene. In agreement with the earlier report,[35] fulleropyrrolidine exhibited a broad emission band at around 712 nm when excited at 390 nm. Changing the wavelength of excitation to other absorption wavelengths of fulleropyrrolidine, revealed no change in the emission maxima. Interestingly, the emission of both the dyad and the triad is found almost completely quenched, indicating the occurrence of excited-state reactions from the singlet excited fulleropyrrolidine. Such efficient quenching is also observed in benzonitrile and acetonitrile solvents. To verify the quenching mechanism and characterize the reaction products, subpicosecond as well as nanosecond transient absorption studies on both the dyad and triad have been performed.

Transient spectral results for the dyad, 2-(ferrocenyl)fulleropyrrolidine, observed after the 150 fs laser excitation at 388 nm in benzonitrile are shown in Figure 6a. Immediately after the laser pulse, a broad transient absorption band appeared in the wavelength region of 800−900 nm and this has been attributed to the singlet−singlet absorption of the fulleropyrrolidine entity.[44] In addition, a sharp band at 970 nm corresponding to the radical anion of the fulleropyrrolidine entity[45] is also observed. A nearly complete decay of both the transient absorption bands is observed after a delay time of 760 ps. As shown in Figure 6b, the rise of the 970 nm band takes place as fast as 10 ps and this may correspond to the occurrence of charge separation from the singlet excited state. From the rise of this band, the evaluated rate of the charge separation generating the ion-pair state is found to be 2.2×10^{11} s^{-1}. The 970 nm band is found to decay with the rate constant of 4.5×10^9 s^{-1}, and this has been ascribed to the charge recombination of the ion-pair state. The residue of the decay at 1000 ps in Figure 6c may be attributed to the tail of the triplet excited state of the fullerene entity, whose absorption maximum may be shorter than 800 nm (spectrum at 760 ps in Figure 6a).

The transient absorption spectra and the time profiles observed after laser excitation of the ferrocene−C_{60}−dinitrobenzene triad are shown in Figure 7a, in which the 970 nm band seen at 4 ps has been attributed to the radical anion of the C_{60} entity.[44] The broad background absorption observed in the whole spectral region has been attributed to the singlet−singlet absorption. At 760 ps, most of the broad singlet−singlet absorption disappears leaving traces of the absorption corresponding to the radical anion of the C_{60} entity at 970 nm and the triplet−triplet absorption at wavelengths shorter than 850 nm. The rise of the 760 nm band is shown in Figure 7b, from which the evaluated charge-separation rate is found to be 2.5×10^{11} s^{-1}. A comparison between the rates obtained for the dyad and the triad suggests that the dinitrobenzene entity slightly accelerates the charge-separation process. The decay rate of the triad estimated from Figure 7c is found to be 8.5×10^9 s^{-1}, which is twice as large as the corresponding rates obtained for 2-(ferrocenyl)fulleropyrrolidine. It is interesting to note that the presence of the dinitrobenzene entity does not slow down the charge-recombination process, although such effect is anticipated from the observed small coefficients of the LUMO on the dinitrobenzene entity (Figure 4b). It may be mentioned here that the dinitrobenzene entity actually assists the charge-separation and charge-recombination processes between ferrocene and fulleropyrrolidine entities upon photoexcitation.

Figure 8 shows the transient absorption spectra observed after nanosecond laser excitation of fulleropyrrolidine and 2-(ferrocenyl)fulleropyrrolidine and *N*-(3′,5′-dinitrobenzoyl)-2-(ferrocenyl)fulleropyrrolidine in benzonitrile. The observed intense transient band of fulleropyrrolidine at 720 nm with a shoulder at 850 nm was attributed to the triplet−triplet absorption, generated via the intersystem crossing from the singlet excited state within 1.2 ns. The intensity of the absorption maximum decays slowly with a rate constant of 1.6×10^5 s^{-1} as shown in the inserted time-profile in Figure 8. In the case of 2-(ferrocenyl)fulleropyrrolidine, the shape of the absorption band is similar to that of fulleropyrrolidine, indicating the formation of the triplet state of the fullerene entity which is also supported by a similar decay rate constant of 2.5×10^5 s^{-1} (inset of Figure 8). However, the absorption intensity is reduced by a factor of about $^1/_8$, suggesting that most of the excited singlet state undergoes the charge-separation process rather than formation of a C_{60} triplet state.

The absorption intensity of the transient absorption band of *N*-(3′,5′-dinitrobenzoyl)-2-(ferrocenyl)fulleropyrrolidine is found to be considerably lower than that of fulleropyrrolidine ($^1/_{60}$). Although the peak at 720 nm is broad, this weak absorption has also been attributed to the triplet state because the lifetime is almost the same as that obtained for fulleropyrrolidine (rate constant = 1.9×10^5 s^{-1}). One of the reasons for the low distribution of the triplet state may be the faster charge-separation process of the triad than that of dyad.

Figure 9 compares the energy level diagrams for the different photochemical events of fulleropyrrolidine, 2-(ferrocenyl)-fulleropyrrolidine and *N*-(3′,5′-dinitrobenzoyl)-2-(ferrocenyl)-fulleropyrrolidine. The high triplet yield in fulleropyrrolidine is attributed to the high quantum yield of intersystem crossing of the singlet excited state (Figure 9a). The observed fast charge-separation rates in the dyad and triad are in good agreement with lower ion-pair states compared with the triplet states. That is, the energy gaps between the singlet excited states and the ion pair states are about 0.5 eV (energy diagrams b and c in Figure 9), which may be normal or top region of the Marcus parabola for fullerene derivatives.[53] This suggests the unlikely formation of a direct triplet state of the fullerene entity via intersystem crossing of the singlet excited state, which is in good agreement with the observed decrease in the formation of the triplet excited state in Figure 8. The faster charge-recombination rate of the ion-pair of the triad compared to that of the dyad could be attributed to spatial back electron transfer from the dinitrobenzene entity to the ferrocene entity. This provides indirect evidence for the migration of the electron toward the dinitrobenzene entity in the ion pair state of the triad, although this process is energetically unfavorable. This unique photochemical and photophysical behavior is further supported by the ab initio calculated distribution of LUMO as shown in Figure 4b.

Summary

Synthesis of a supramolecular triad comprised of three redox active entities, namely, ferrocene, C_{60}, and dinitrobenzene, has been accomplished. Electrochemical studies revealed multiple redox processes involving all three redox active entities. The observed eight reversible redox couples within the accessible potential window of *o*-dichlorobenzene suggest that fullerene bearing redox active groups which undergo reversible redox reactions may be more suitable for building molecular charge storage devices than pristine fullerenes. Computational calculations performed using the ab initio B3LYP/3-21G(*) method predicted a plausible geometry and electronic structure of the investigated triad, whereas such calculations performed by semiempirical PM3 or Hartree−Fock 3-21G(*) revealed either an incorrect geometry or incorrect electronic structure which did not agree with the experimental observations. The calculated HOMO orbital by the B3LYP/3-21G(*) method was found to lie primarily on the ferrocene entity, whereas the LUMO orbitals are mainly located on the C_{60} entity with small orbital coefficients on the dinitrobenzene entity. The orbital coefficients of the subsequent LUMO orbitals track the observed site of electrochemical reductions of the triad. Both steady-state fluorescence and time-resolved picosecond transient absorption studies revealed efficient charge separation and charge recombination in the studied triad, and this has been attributed to the close spacing of the entities of the triad to one another. The estimated rise and decay rate constants are found to be slightly higher for the triad as compared to the corresponding rates of the dyad.

Acknowledgment. The authors are thankful to the donors of the Petroleum Research Fund, administered by the American Chemical Society, National Institutes of Health, National Science Foundation CCLI and A&I (to FD), and the Dreyfus Foundation (to MES) for support of this work. The authors are also thankful to the High Performance Computing Center of the Wichita State University for lending SGI ORIGIN 2000 computer time.

Supporting Information Available: The ESI−mass spectra in CH_2Cl_2 matrix, UV−visible spectra in *n*-hexane, and ^{1}H NMR spectra in $CDCl_3/CS_2$ (1:1 v/v) of 2-(ferrocenyl)fulleropyrrolidine and *N*-(3′5′-dinitrobenzoyl)-2-(ferrocenyl)-fulleropyrrolidine. This material is available free of charge via the Internet at http://pubs.acs.org.

References and Notes

(1) Martin, N.; Sachez, B.; Illescas, B.; Perez, I. *Chem. Rev*. **1998**, *98*, 2427.
(2) Prato, M.; Maggini, M. *Acc. Chem. Res*. **1998**, *31*, 519.
(3) Carano, M.; Ceroni, P.; Paolucci, F.; Roffia, S.; Da Ros, T.; Prato, M.; Sluch, M. I.; Pearson, C.; Petty, M. C.; Bryce, M. R. *J. Mater. Chem*. **2000**, *10*, 269.
(4) *Fullerene and Related Structures*; Hirsch, A., Ed.; Springer: Berlin, 1999; Vol. 199.
(5) Long, N. J. *Angew. Chem., Int. Ed. Engl*. **1995**, *34*, 21.
(6) *Molecular Electronic-Science and Technologie*; Aviram, A., Ed.; Engineering Foundation: New York, 1989.
(7) Aviram, A.; Ratner, M. *Chem. Phys. Lett*. **1974**, *29*, 277.
(8) Launay, J. P. In *Molecular Electronics in Granular Nanoelectronics*; Ferry, D. K., Ed.; New York, 1995.
(9) *Introduction to Molecular Electronics*; Petty, M. C., Bryce, M. R., Bloor, D., Eds.: Oxford University Press: New York, 1995.
(10) Prasad, P. N.; Williams, D. J. *Introduction to Nonlinear Optical Effects in Molecules and Polymers*; Wiley: New York, 1991.
(11) Nalwa, M. S. *Adv. Mater*. **1993**, *5*, 341.
(12) *Photoinduced Electron Transfer*; Fox, M. A., Channon, M., Eds.; Elsevier: Amsterdam, 1988; Parts A−D.
(13) Kurreck, H.; Huber, M. *Angew. Chem., Int. Ed. Engl*. **1995**, *34*, 849.
(14) Staab, H. A.; Feurer, A.; Hauck, R. *Angew. Chem., Int. Ed. Engl*. **1994**, *33*, 2428.
(15) Roest, M. R.; Verhoeven, J. W.; Schiddeboon, W.; Warman, J. M.; Lawson, J. M.; Paddon-Row, M. N. *J. Am. Chem. Soc*. **1996**, *118*, 1762.
(16) Maruyama, K.; Osuka, A. *Pure Appl. Chem*. **1990**, *62*, 1511.
(17) Gust, D.; Moore, T. A. *Science* **1989**, *244*, 35.
(18) (a) Gust, D.; Moore, T. A. *Top. Curr. Chem*. **1991**, *159*, 103. (b) Gust, D.; Moore, T. A.; Moore, A. L. *Pure Appl. Chem*. **1998**, *70*, 2189.
(19) Gust, D.; Moore, T. A.; Moore, A. L. *Acc. Chem. Res*. **1993**, *26*, 198.
(20) Wasielewski, M. R. *Chem. Rev*. **1992**, *92*, 435.
(21) Paddon-Row, M. N. *Acc. Chem. Res*. **1994**, *27*, 18.
(22) Sutin, N. *Acc. Chem. Res*. **1983**, *15*, 275.
(23) Bard, A. J.; Fox, M. A. *Acc. Chem. Res*. **1995**, *28*, 141.
(24) Meyer, T. J. *Acc. Chem. Res.* **1989**, *22*, 163.
(25) Piotrowiak, P. *Chem. Soc. Rev*. **1999**, *28*, 143.
(26) Imahori, H.; Sakata, Y. *Adv. Mater*. **1997**, *9*, 537.
(27) Diederich, F.; Gomez-Lopez, M. *Chem. Soc. Rev*. **1999**, *28*, 263.
(28) Guldi, D. M. *Chem. Commun*. **2000**, 321.
(29) (a) Liddell, P. A.; Kuciauskas, D.; Sumida, J. P.; Nash, B.; Nguyen, D.; Moore, A. L.; Moore, T. A.; Gust, D. *J. Am. Chem. Soc*. **1997**, *119*, 1400. (b) Kuciauskas, D.; Liddell, P. A.; Lin, S.; Johnson, T. E.; Wighorn, S. L.; Lindsey, J. S.; Moore, A. L.; Moore, T. A.; Gust, D. *J. Am. Chem. Soc*. **1999**, *121*, 8604. (c) Carbonera, D.; Di Valentin, M.; Corvaja, C.; Agostini, G.; Giacometti, G.; Liddell, P. A.; Kuciauskas, D.; Moore, A. L.; Moore, T. A.; Gust, D. *J. Am. Chem. Soc*. **1998**, *120*, 4398.
(30) Luo, C.; Guldi, D. M.; Imahori, H.; Tamaki, K.; Sakata, Y. *J. Am. Chem. Soc*. **2000**, *122*, 6535.
(31) D'Souza, F.; Deviprasad, G. R.; El-Khouly, M. E.; Fujitsuka, M.; Ito, O. *J. Am. Chem. Soc*. **2001**, *123*, 5277−5284 and references therein.
(32) Maggini, M.; Karlsson, A.; Scorrano, G.; Sandona, G.; Farnia, G.; Prato, M. *J. Chem. Soc., Chem. Commun*. **1994**, 589.
(33) Prato, M.; Maggini, M.; Giacometti, C.; Scorrano, G.; Sandona, G.; Farnia, G. *Tetrahedron* **1996**, *52*, 5221.
(34) Noworyta, K.; Krinichnaya, E. P.; Kutner, W.; Smith, P. M.; Deviprasad, G. R.; D'Souza, F. Fullerenes 2000: Electrochemistry and Photochemistry. *Proc. Electrochem. Soc*. **2000**, *8*, 54; Fukuzumi, S., D'Souza, F., Guldi, D. M., Eds.

(35) Guldi, D. M.; Maggini, M.; Scorrano, G.; Prato, M. *J. Am. Chem. Soc*. **1997**, *119*, 974.

(36) Poplawska, M.; Byszewski, P.; Kowalska, E.; Diduszko, R.; Radomska, J. *Synth. Met.* **2000**, *109*, 239.

(37) Deviprasad, G. R.; Rahman, M. S.; D'Souza, F. *Chem. Commun*. **1999**, 849.

(38) de la Cruz, P.; de la Hoz, A.; Langa, F.; Martin, N.; Perez, M. C.; Sanchez, L. *Eur. J. Org. Chem*. **1999**, 3433.

(39) Maggini, M.; Scorrano, G.; Prato, M. *J. Am. Chem. Soc*. **1993**, *115*, 9798.

(40) Frisch, M. J.; Trucks, G. W.; Schlegel, H. B.; Scuseria, G. E.; Robb, M. A.; Cheeseman, J. R.; Zakrzewski, V. G.; Montgomery, J. A., Jr.; Stratmann, R. E.; Burant, J. C.; Dapprich, S.; Millam, J. M.; Daniels, A. D.; Kudin, K. N.; Strain, M. C.; Farkas, O.; Tomasi, J.; Barone, V.; Cossi, M.; Cammi, R.; Mennucci, B.; Pomelli, C.; Adamo, C.; Clifford, S.; Ochterski, J.; Petersson, G. A.; Ayala, P. Y.; Cui, Q.; Morokuma, K.; Malick, D. K.; Rabuck, A. D.; Raghavachari, K.; Foresman, J. B.; Cioslowski, J.; Ortiz, J. V.; Stefanov, B. B.; Liu, G.; Liashenko, A.; Piskorz, P.; Komaromi, I.; Gomperts, R.; Martin, R. L.; Fox, D. J.; Keith, T.; Al-Laham, M. A.; Peng, C. Y.; Nanayakkara, A.; Gonzalez, C.; Challacombe, M.; Gill, P. M. W.; Johnson, B. G.; Chen, W.; Wong, M. W.; Andres, J. L.; Head-Gordon, M.; Replogle, E. S.; Pople, J. A. *Gaussian 98*, revision A.7; Gaussian, Inc.: Pittsburgh, PA, 1998.

(41) *SPARTAN* PRO; Wavefunction, Inc.: Irvine, CA 92715.

(42) *Cache MOPAC*-2000, version 4.4; Fujitsu Systems, Inc.: http://www.cachesoftware.com.

(43) (a) Matsumoto, K.; Fujitsuka, M.; Sato, T.; Onodera, S.; Ito, O. *J. Phys. Chem. B* **2000**, *104*, 11632. (b) Komamine, S.; Fujitsuka, M.; Ito, O.; Morikawa, K.; Miyata, T.; Ohno, T. *J. Phys. Chem. A* **2000**, *104*, 11497.

(44) Nojiri, T.; Watanabe, A.; Ito, O. *J. Phys. Chem. A* **1998**, *102*, 5215.

(45) Fujitsuka, M.; Ito, O.; Yamashiro, T.; Aso, Y.; Otsubo, T. *J. Phys. Chem. A* **2000**, *104*, 4876.

(46) Kutner, W.; Noworyta, K., Deviprasad, G. R.; D'Souza, F. *J. Electrochem. Soc*. **2000**, *147*, 2647.

(47) Xie, Q.; Perez-Cordero, E.; Echegoyen, L. *J. Am. Chem. Soc*. **1992**, *114*, 3978.

(48) (a) Hehre, W. J. *Practical Strategies for Electronic Structure Calculation*; Wavefunction, Inc.: Irvine, CA, 1996. (b) Hehre, W. J. *Critical Assessment of Modern Electronic Structure Methods*; Wavefunction, Inc.: Irvine, CA, 1995.

(49) D'Souza, F.; Zandler, M. E.; Deviprasad, G. R.; Kutner, W. *J. Phys. Chem. A* **2000**, *104*, 6887.

(50) D'Souza, F.; Rath, N. P.; Deviprasad, G. R.; Zandler, M. E. *Chem. Commun*. **2001**, 267.

(51) Stowasser, R.; Hoffmann, R. *J. Am. Chem. Soc*. **1999**, *121*, 3414.

(52) (a) Brown, S. T.; Rienstra-Kiracofe, J. C.; Schaefer, H. F. *J. Phys. Chem. A* **1999**, *103*, 4065. (b) Rienstra-Kiracofe, J. C.; Barden, C. J.; Brown, S. T.; Schaefer, H. F. *J. Phys. Chem. A* **2001**, *105*, 524.

(53) Imahori, H.; Tamaki, K.; Gulidi, D. M.; Luo, C.; Fujitsuka, M.; Ito, O.; Sakata, Y.; Fukuzumi, S. *J. Am. Chem. Soc*. **2001**, *123*, 2607.